LNF-88/73

N. Cavallo, F. Cevenini, M.R. Masullo, M. Castellano, S. Guiducci, P. Patteri, M.A Preger, M. Serio

FINAL REPORT ON THE LELA EXPERIMENT

Estratto da: Nucl. Instr. & Meth. in Phys. Res. A272, 64 (1988)

Nuclear Instruments and Methods in Physics Research A272 (1988) 64–67
North-Holland, Amsterdam

FINAL REPORT ON THE LELA EXPERIMENT

Nicola CAVALLO, Francesco CEVENINI and Maria Rosaria MASULLO

Istituto Nazionale di Fisica Nucleare, Sezione di Napoli, and
Dipartimento di Fisica Nucleare, Struttura della Materia e Fisica Applicata dell'Università di Napoli, Napoli, Italy

Michele CASTELLANO, Susanna GUIDUCCI, Piero PATTERI, Miro Andrea PREGER and Mario SERIO

Istituto Nazionale di Fisica Nucleare, Laboratori Nazionali di Frascati, Italy

Progress in the LELA (free electron laser on ADONE) experiment from September 1986 to July 1987 is described. Improvements in machine lattice and control, and automation in cavity alignment allowed for a maximum Q factor of $\approx 10^3$.

1. Introduction

The LELA experiment was proposed [1] in 1981 to study the feasibility and the limits of an FEL built on an existing machine (the Frascati storage ring ADONE). Since then an electromagnetic plane undulator has been built [2] and its spontaneous radiation carefully studied [3]. Stimulated emission has been measured both in the fundamental and the third harmonic [4], and during the last years a peculiar optical cavity has been built and operated [5]. The measured peak gain being $\approx 3 \times 10^{-4}$, an upgrade in the machine performance was planned for Summer 1986, which could improve this value.

Between January and May 1987 we used the last available shifts to carry on the experimental program as far as possible, exploiting the experience gained in cavity alignment during 1986 runs.

2. Machine diagnostics

The diagnostic and control system of the ADONE storage ring has been largely improved by the machine group in 1986. Button-type position monitors and on-line orbit correction have been implemented [6]. These greatly helped to realize a new magnetic lattice with vanishing dispersion in the undulator straight section. Furthermore the on-line orbit correction assured a good reproducibility and stability of the radiation axis between successive injections.

The reproducibility of the measurement at each point is within a few tens of microns. Before the first alignment of the cavity the closed orbit distortion is iteratively corrected. This procedure brings the beam trajectory well within the tolerance required by our experiment but it requires several minutes. Closed orbit errors ≤ 100 μrad and ≤ 300 μm were measured when the same correction set was used for the successive injections. This is obviously less time consuming than repeating the correction procedure after each accumulation.

The cavity axis, which must overlap the electron trajectory in the undulator within 0.1 mm, was aligned with the radiation after orbit correction. The fine control of the transverse alignment, actuated by piezoelectric pushers (PZTs), correct the residual errors. When the PZT limit was approached, a new correction set was established.

The new machine lattice was especially designed to provide a smaller transverse beam size to get the best overlap between the cavity mode and the electron beam envelope. Its main feature is vanishing dispersion in the undulator straight section. A measurement of the beam displacement induced by a known change in rf frequency, proportional to the disperison η, is shown in fig. 1 (pickups are missing in positions 11–20–21).

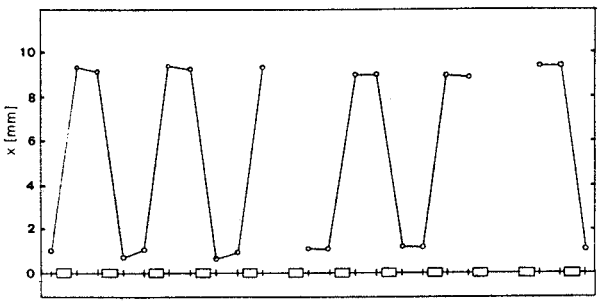

Fig. 1. Difference between horizontal position of the beam with $f_{rf} = 51.405$ MHz and $f_{rf} = 51.410$ MHz.

Unfortunately the new lattice has a momentum compaction factor smaller by a factor 4 than the normal one, and the thresholds for instabilities showed up to be much lower: they could not be cured with the present feedback system preventing us to operate the storage ring at high current, as would be required to reach a gain $\geq 1 \times 10^{-3}$.

We decided to continue using the standard machine lattice, which allows for a maximum gain of $\approx 3 \times 10^{-4}$. Some advantages were expected from the replacement of the old vacuum chamber by a new one. Although at low current a much shorter bunch length was observed, the usual length increase was observed at larger current. This behaviour did not fit easily any bunch lengthening model: even if the threshold for the microwave instability was larger than before by a factor $\cong 3$, at the design current ($\cong 100$ mA in 3 bunches) the measured bunch length was not small enough to increase the gain value substantially.

3. Alignment improvement and automation

During the 1986 runs a rather fast mirror reflectivity degradation rate has been measured (3×10^{-5} $mA^{-1}\,h^{-1}$) although a number of counteractions were taken to reduce it [7]. The reflectivity losses were mainly attributed to bulk damage since the very low level of carbon density in the residual gas ruled out carbon surface contamination. Thick lead walls were placed outside the cavity pipe wherever possible to stop the high energy radiation, mainly coming from the injection losses impinging on the mirrors, so we attribute the damage to the ultraviolet radiation from the higher harmonics of the undulator and to high energy radiation coming from the machine on the cavity axis: the latter is mainly caused by bremsstrahlung of electrons on the residual gas in the long (≈ 6 m) straight section, which cannot be avoided in the high energy operation of the ring for other experiments, since a sufficiently thick beam stopper in the cavity has not been provided. It has been estimated that the cavity Q could be kept > 1000 for no longer than 30 min at the maximum current which could be stored in the machine. This pushed us to realize a fast alignment procedure to have as minimum as possible integrated current in the machine after the mirrors are installed in the cavity. A mirror change during our shift time was successfully attempted: this assured that no useless irradiation was suffered by the mirror, at the price of an appreciable fraction of our machine time.

The preliminary alignment and the fine transverse tuning, both requiring long iterative procedures or scanning, were performed. The most time consuming operation in the preliminary alignment procedure was centering the upstream mirror and alignment of the external laser on the same undulator axis. Since no reference on direct radiation was available before the undulator, the laser had to be aligned on the radiation axis after the upstream mirror. Then the mirror center was moved on the laser axis. Since the plane-concave mirror glass acted as a deflecting wedge for rays passing off-axis through the mirror, a long iterative procedure had to be applied. These alignments often showed to be unsatisfactory at the following step to get a high Q cavity but the error could be detected only with radiation inside the cavity, when mirror damage already started.

In the 1987 runs a 30 m radius mirror has been placed on the radiation cone, nearly 25 m downstream of the undulator. The undulator radiation spot, focused near the upstream mirror, is a clear reference for its positioning. An iris placed just after the exit window is used to collimate both the direct and the reflected radiation beams. The axis of the radiation reflected back by the concave mirror can be aligned on the direct axis with small angular error, owing to the long distance between the iris and the concave mirror. When the laser beam is aligned on the radiation axis after this setting, a reliable line is available for the preliminary transverse alignment of the cavity and then it is possible to easily get a satisfactory rough alignment.

The fine tuning procedure, aiming at maximizing the stored radiation intensity, was performed satisfactorily in the 1986 runs. The main effort has been devoted to automate it and to speed up each step of the operation. The setup for the automatic alignment is shown in fig. 2. Iris I_1 is placed close to the exit of the downstream optical cavity window, in order to eliminate the intense

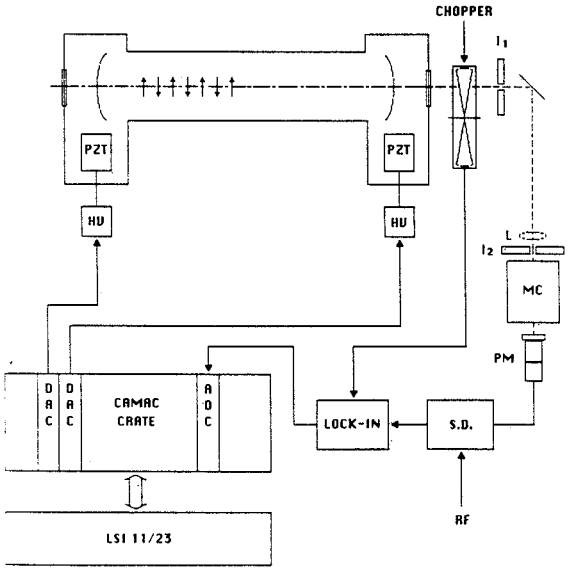

Fig. 2. Layout of the alignment optimization system.

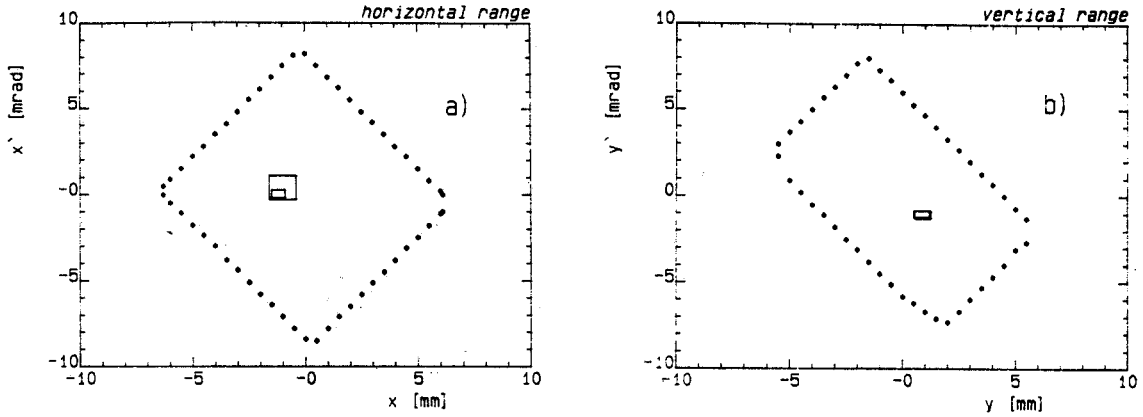

Fig. 3. Horizontal and vertical range in X, X' plane of the cavity axis with pushers. Inner rectangles show the sweeping range of an alignment procedure.

stray rays passing outside the mirror. Lens L is used to optimize the wavelength resolution of the monochromator.

Another critical step was centering the detector on the downstream radiation axis for cavity tuning operation. The spectral and spatial distribution of this beam was mainly determined by the mirror reflectivity band, so that the characteristic annular structure of the undulator radiation was blurred. The peak wavelength was searched for by scanning the monochromator with iris I_2 full open and with the upstream mirror completely tilted to avoid unwanted light round trips. The iris was then partially closed and its position was optimized to maximize the peak intensity. This guarantees that the fine alignment will maximize radiation accumulation along the right axis.

A synchronous demodulation system was used to extract the low frequency modulated signal from the chopped light pulse train. The noisy signal of the PM was filtered by a lock-in amplifier and detected via a CAMAC ADC. At the same time the intensity of the current stored in the ring was recorded to normalize the cavity signal.

The cavity mirror movements were actuated by the PZT pushers. Their hv drivers were controlled via CAMAC DACs by the computer, as shown in fig. 2.

PZT operation is reliable and reproducible if they all move along the same hysteresis path. The decreasing side of the cycle is better suited to a simple parabolic fit of PZT length vs voltage. In this way complete control of the optical axis was achieved. The range obtainable by the PZT pushers is shown in fig. 3. The area within dots represents the range of movements for the PZT, while the small rectangles show the range in which a typical fine alignment procedure is performed.

Laboratory tests showed that the cycle speed was mainly limited by the hv driver internal resistance when discharging the PZT capacitance to ground. An external load resistor speeded up the cycle so that the settling time due to mirror movements did not cause significant delay in scanning. The time delay between successive

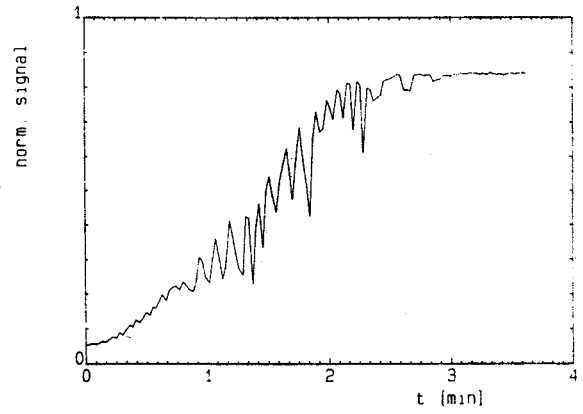

Fig. 4. Light intensity measurement during the automatic cavity alignment procedure.

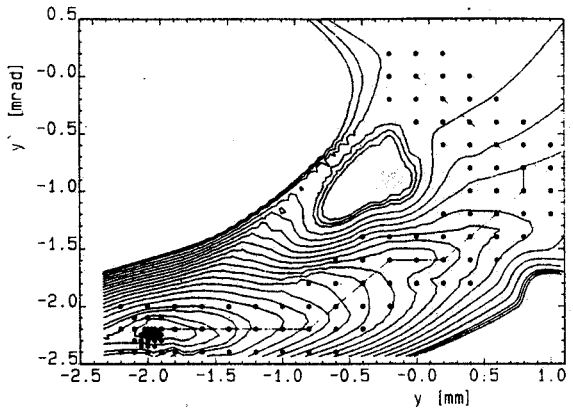

Fig. 5. Cavity axis path during an alignment procedure.

points is mainly set by the time constant of the lock-in amplifier.

The program moved the cavity axis in one plane at a time. The initial positions and slopes of the optical axis, in both planes, were defined with the PZTs at half range. Eight equally spaced points in the phase space X, X' around the central one were tested and the axis was moved where the highest signal was measured. The procedure was repeated until a maximum was found, then the step sizes were halved and the whole procedure restarted. The same operation was performed for the other plane. Typical final step sizes after three iterations were $\Delta X = 25\ \mu$m and $\Delta X' = 25\ \mu$rad.

The light intensity measurements during the alignment procedure are sequentially plotted in fig. 4. The corresponding path of the cavity axis in the X, X' plane is shown in fig. 5. The signal level curves have been drawn using a standard contouring approximation performing a bidimensional fit.

In order to check that cavity alignment could be performed before significant reduction of mirror reflectivity by radiation damage, a new set of mirrors was placed in the cavity, and the alignment procedure started before the mirrors were exposed to any possible radiation. A maximum accumulation factor (radiation sorted in the cavity divided by the spontaneous radiation emitted during a single passage of the beam in the undulator) of 10^3 was measured, corresponding to a single mirror loss of $\approx 5 \times 10^{-4}$.

The longitudinal tuning requires careful measurement of the cavity length, which cannot be obtained by mechanical means. If the cavity length is slightly different from the electron bunch spacing and the Q is high, the cavity light pulse will exhibit a tail on the leading or the trailing edge, owing to the different round-trip times of electron bunches and light pulses.

Fig. 6 shows an example of the shape of the signal pulses for several displacements of the downstream mirror. Curves (a) and (b), differing by 0.1 mm, are very close to the optimal length of the cavity resonator, while curve (c) represents a too long cavity.

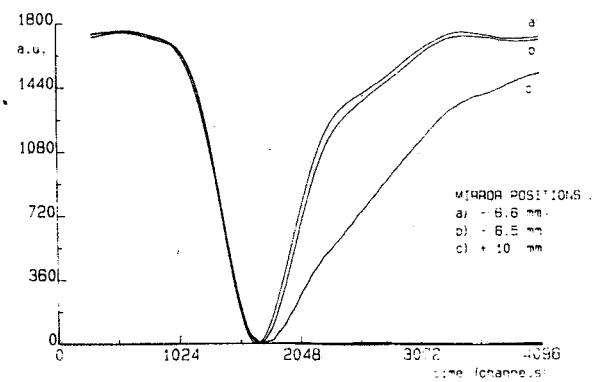

Fig. 6. Shape of light pulses at different cavity lengths.

A set of measurements corresponding to different mirror displacements, with a step size of 0.1 mm, has been performed. These points have been chosen to be near the position that, referring to a previous set of measurements performed with a larger step size, corresponds approximately to the optimal cavity length.

The slope α of the tail, after deconvolution of data points to take into account the risetime of the acquisition device, is related to the cavity length error ΔL by $\Delta L = (1/\alpha)Q$. The mirror position was estimated by means of a linear fit with an error of ± 0.2 mm.

After moving the mirror to this position a closer scanning was carried out with a micrometric movement in 0.1 mm steps. Unfortunately this mechanical movement worsened the transverse alignment quality, and a new optimization had to be performed at each step.

No clear evidence of stimulated emission could be seen. Actually the mechanical step was larger than the detuning curve width, but the aforementioned operations were time consuming and a complete scan at closer steps could not be completed before the mirrors were strongly damaged.

The longitudinal tuning was also attempted by moving the rf frequency of the storage ring. In ADONE $f_{rf} = 51.411$ MHz, harmonic number $h = 18$ and $L_{orbit} = 105$ m, so that an equivalent lengthening $\delta L = L\delta f/f = 2\ \mu$m/Hz was possible, producing a negligible transverse displacement. A frequency sweep $\Delta f = \pm 200$ Hz was possible before the onset of instabilities. This range corresponds to $\delta L = \pm 0.2$ mm, i.e. the same size as the estimated error in position.

We tried to detect the deformation of the spontaneous radiation spectrum, which might appear also at low gain, but this attempt was unsuccessful. Due to a machine shutdown starting in July 1987, no further attempts were possible.

References

[1] R. Barbini and G. Vignola, in: Physics of Quantum Electronics, vol. 8 (1980) p. 235.
[2] R. Barbini et al., Nucl. Instr. and Meth. 190 (1981) 159.
[3] M. Castellano et al., Nuovo Cim. 81B (1984) 67;
M. Castellano et al., Nucl. Instr. and Meth. A239 (1985) 235.
[4] R. Barbini et al., J. Phys. Coll. C1, 44 (1983) 1;
M. Biagini et al., SPIE Proc. 453 (1983) 275.
[5] M. Ambrosio et al., INFN/TC-84/9 (1984);
M. Biagini et al., Nucl. Instr. and Meth. A237 (1985) 273;
M. Ambrosio et al., Nucl. Instr. and Meth. A246 (1985) 63.
[6] A. Aragona et al., Proc. Particle Accelerator Conf., Washington (1987).
[7] M. Ambrosio et al., Nucl. Instr. and Meth. A250 (1986) 239, 289;
P. Patteri et al., Nucl. Instr. and Meth. A259 (1987) 88.